Supporting Information

Effect of dz^2 Orbital Electron-Distribution of La-Based Inorganic Perovskites on Surface Kinetics of a Model Reaction

Yamkela Nzuzo[a], Adedapo Adeyinka[a], Emanuela Carleschi[b], Bryan P. Doyle[b], Ndzondelelo Bingwa[a*]

Research Centre for Synthesis and Catalysis, Department of Chemical Sciences, University of Johannesburg, PO Box 524, Johannesburg, South Africa.

[b]*Department of Physics, University of Johannesburg, PO Box 524, Johannesburg, South Africa.*

email: nbingwa@uj.ac.za

Table S1: Calculated Goldschmidt's tolerance factors for Lanthanum-based perovskites.

Entry	Catalyst	Tolerance factor (t)
1.	$LaCrO_3$	0.89
2.	$LaMnO_3$	0.86
3.	$LaFeO_3$	0.91
4.	$LaCoO_3$	0.87
5.	$LaNiO_3$	0.94
6.	$LaCuO_3$	0.75
7.	$LaZnO_3$	0.99

TPR Analysis

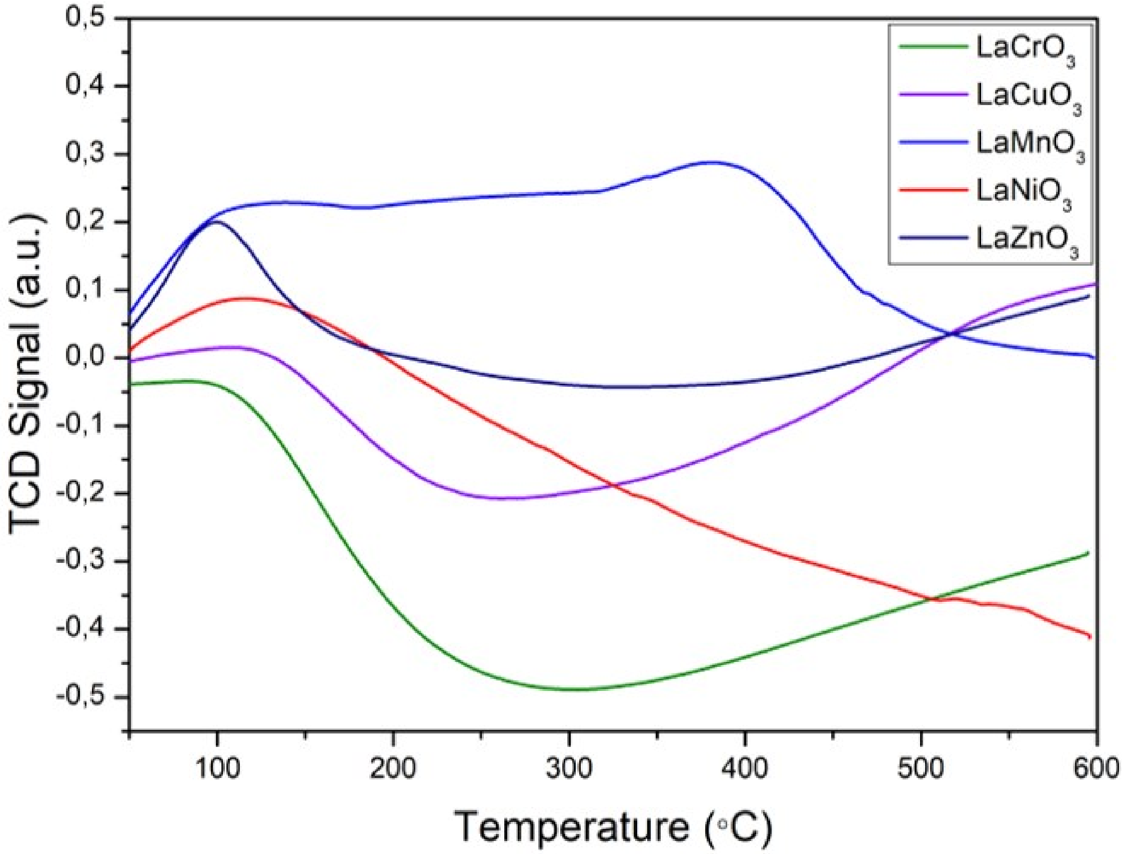

Figure S1: TPR profiles of the perovskites.

TGA Analysis

The obtained surface areas for synthesized perovskites are relatively low, it is clearly that the surface area is not only a determining factor for its higher catalytic activity. We postulated that the stability was also a key factor to the higher catalytic efficiency of a catalyst. The $LaMO_3$ perovskites showed higher stability and degradation was observed in 2 steps. The first step is ascribed to the loss of water molecules and the second step is ascribed to total decomposition of the organic in the perovskite catalysts.

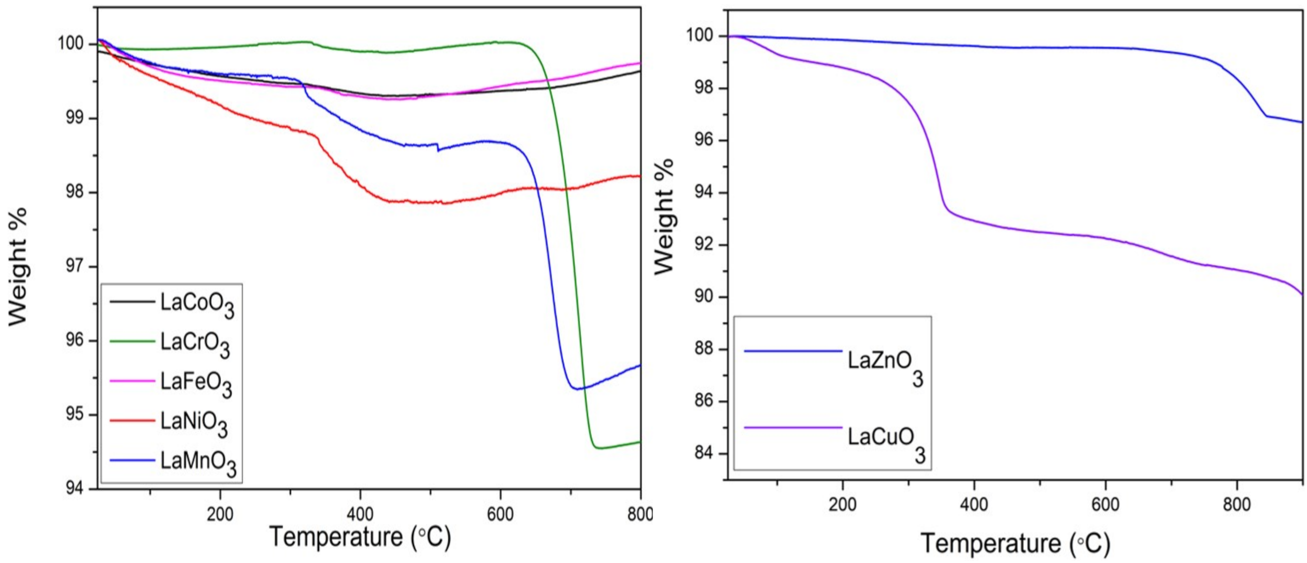

Figure S2: TGA profiles of $LaMO_3$ (M= Co, Cr, Fe, Ni, Mn, Cu, Zn) perovskites.

SEM and TEM Analysis

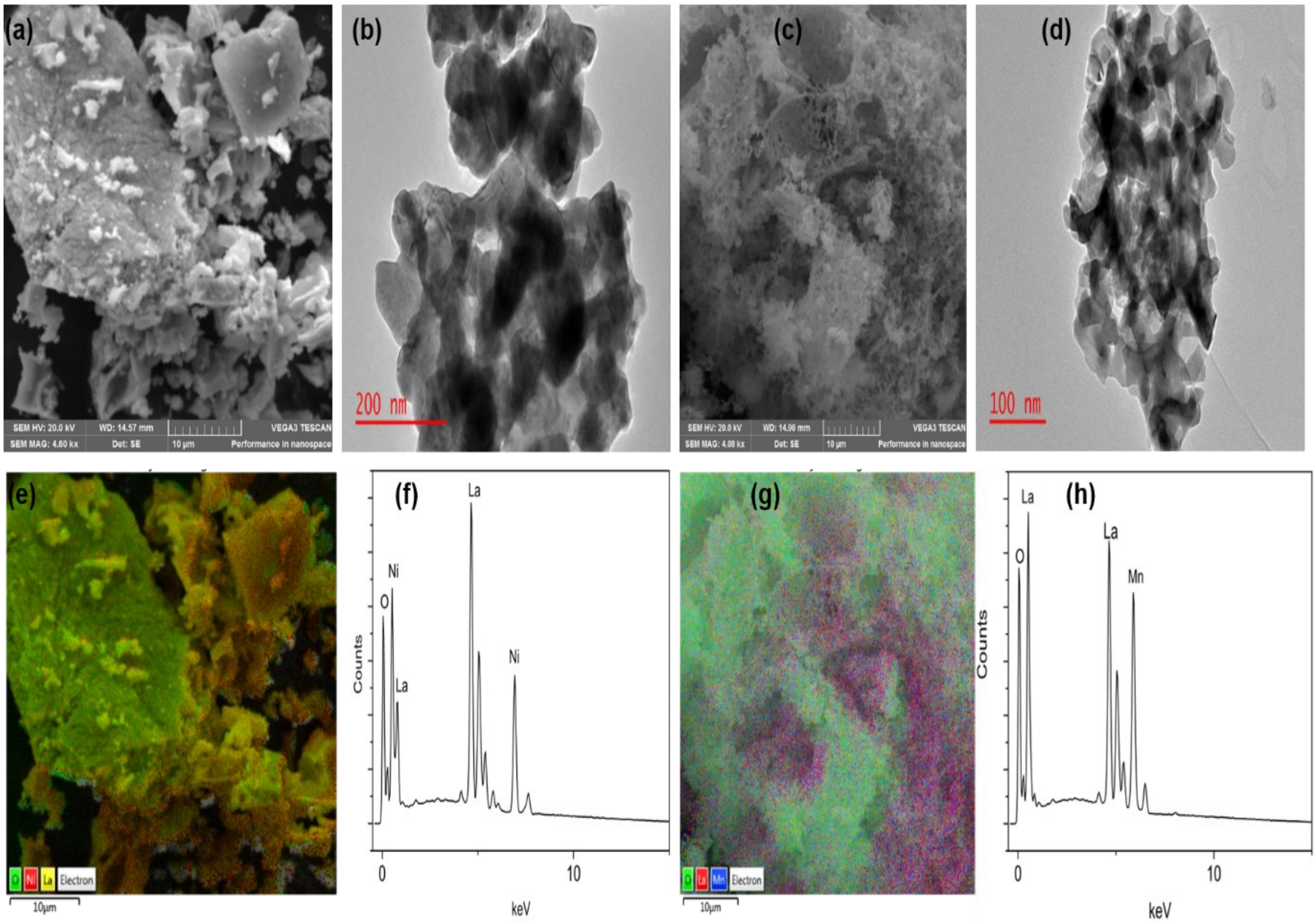

Figure S3: (a) SEM image and (b) TEM image for $LaNiO_3$; (c) SEM image and (d) TEM image for $LaMnO_3$; (e) Elemental mapping and (f) EDS spectrum for $LaNiO_3$; (g) Elemental mapping and (h) EDS spectrum for $LaMnO_3$.

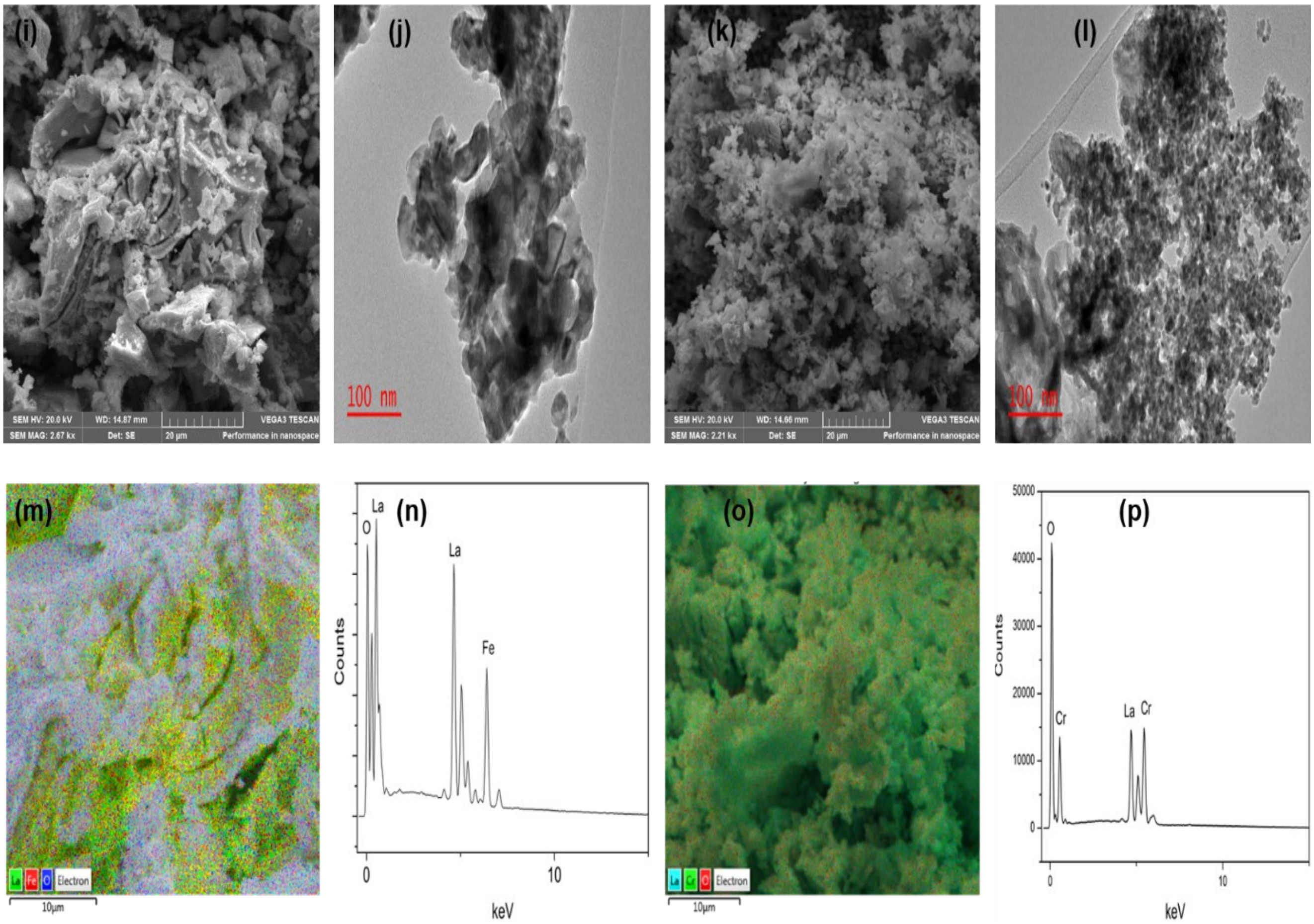

Figure S4: (i) SEM image and (j) TEM image for $LaFeO_3$ (k) SEM image and (l) TEM image for $LaCrO_3$ (m) Elemental mapping and (n) EDS spectrum for $LaFeO_3$ (o) Elemental mapping and (p) EDS spectrum for $LaCrO_3$.

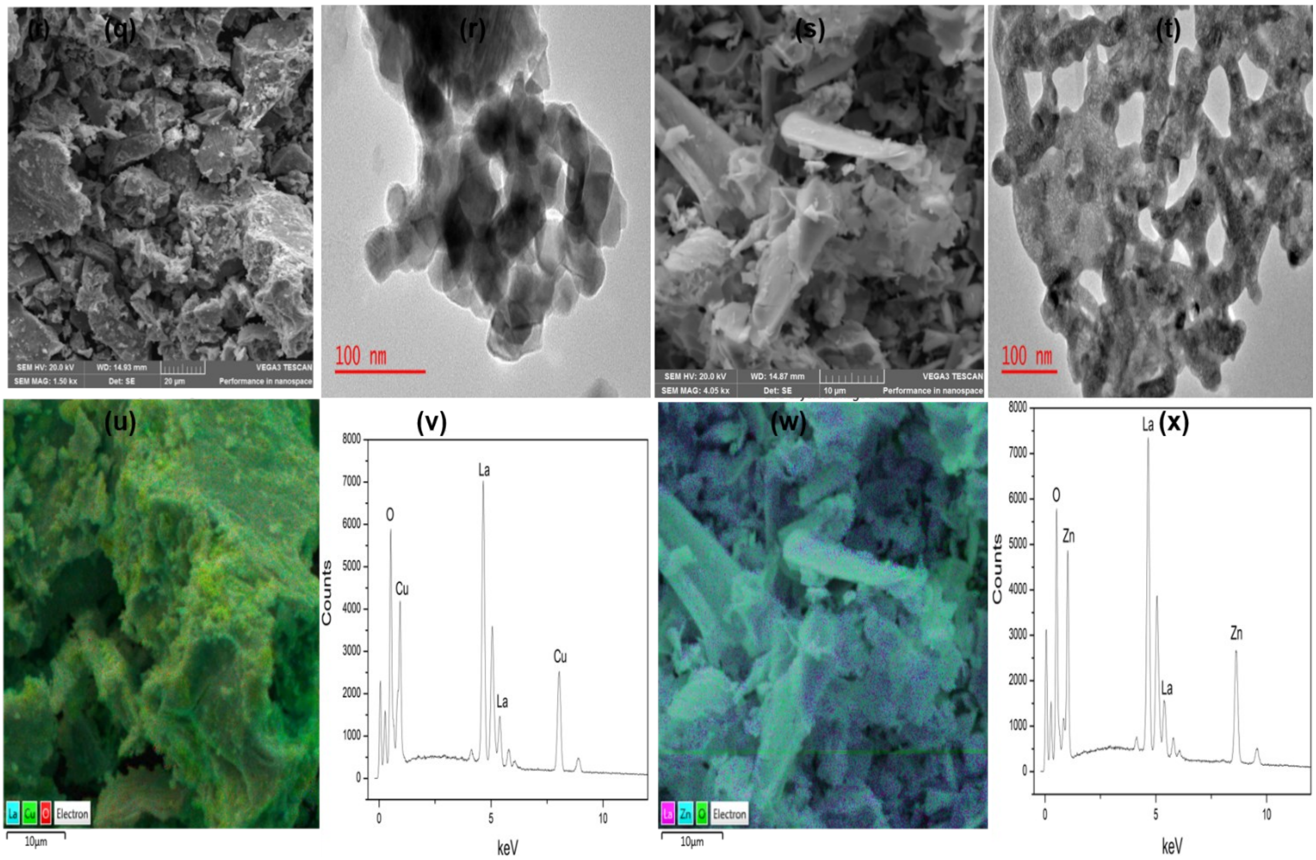

Figure S5: (q) SEM image and (r) TEM image for $LaCuO_3$ (s) SEM image and (t) TEM image for $LaZnO_3$ (u) Elemental mapping and (v) EDS spectrum for $LaCuO_3$ (w) Elemental mapping and (x) EDS spectrum for $LaZnO_3$.

Catalytic Reactions

Morin concentration variation

Morin concentration was carried out to investigate the effect of concentration on the surface of morin while fixing H_2O_2 concentration. Concentration range (50-250 μM) was used. Based on the results obtained, the absorbance decreases as the morin concentration increases. This may be due to the concentration of morin on the surface of the catalyst. At the surface of the catalyst, the morin and H_2O_2 were adsorbed before the reaction. So, as the morin concentration increases catalyst surface area would be covered with morin, therefore less morin will be absorbed to the surface which makes it very for H_2O_2 to be adsorbed on the active site of the catalyst thereby decreases the rate of reaction [1]. Moreover, the observed rate of reaction decreases as the morin concentration increases.

Hydrogen peroxide variation

The reaction rate (k_{obs}) was measured while varying the concentration of hydrogen peroxide at room temperature. The concentration increases as k_{obs} increases thereby gives positive correlation. These results are in good agreement with MnO_x nanoparticles catalyzed the oxidation of morin [2].

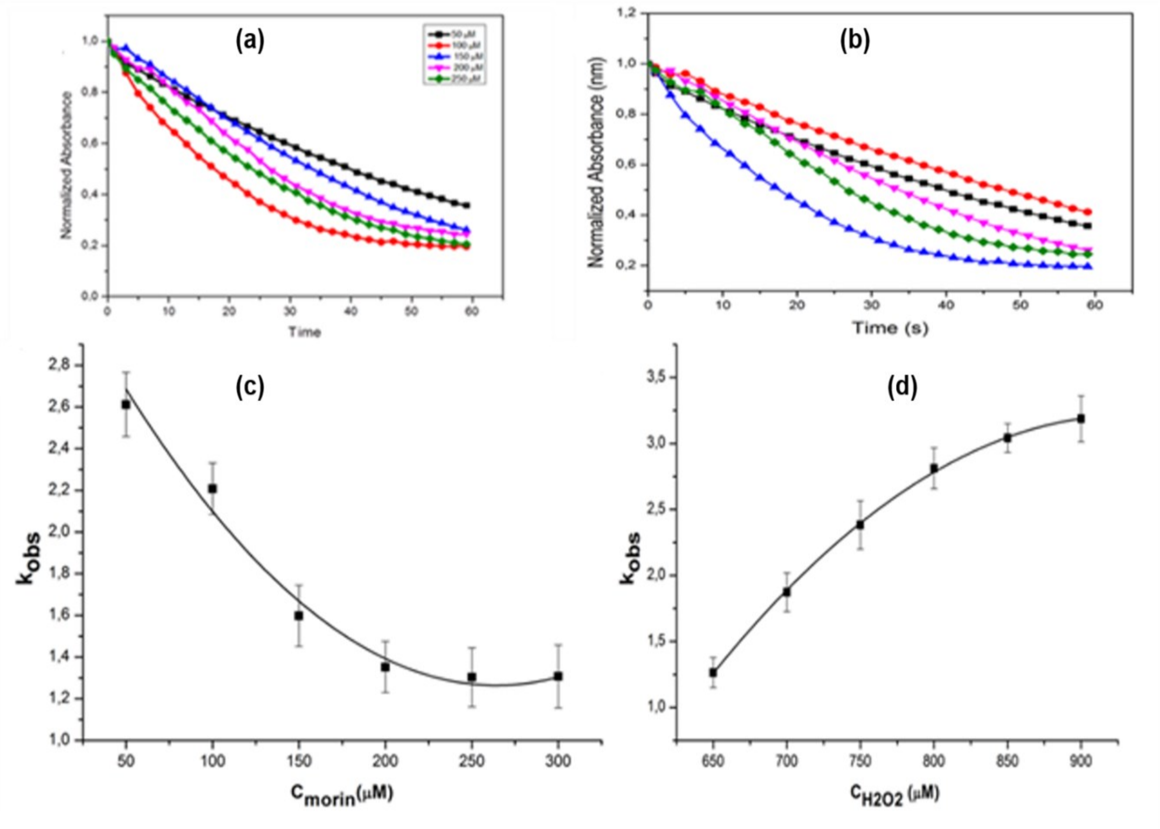

Figure S6: The relationship between **(a)** Absorbance vs time, **(b)** Absorbance vs time **(c)** k_{obs} vs [morin] and **(d)** k_{obs} vs [H_2O_2].

Table S3: Calculated rate of reaction for concentration variation.

Morin concentration (µM)	**Catalyst**	**Rate (S^{-1})**
250	$LaCrO_3$	5.267×10^{-1}
200	$LaCrO_3$	6.180×10^{-1}
150	$LaCrO_3$	5.118×10^{-1}
100	$LaCrO_3$	4.808×10^{-1}
50	$LaCrO_3$	3.830×10^{-1}
H_2O_2 concentration (µM)	**Catalyst**	**Rate (S^{-1})**
900	$LaCrO_3$	2.581×10^{-1}
850	$LaCrO_3$	2.814×10^{-1}
800	$LaCrO_3$	2.678×10^{-1}
750	$LaCrO_3$	3.932×10^{-1}
700	$LaCrO_3$	5.271×10^{-1}

Adsorption Energies results

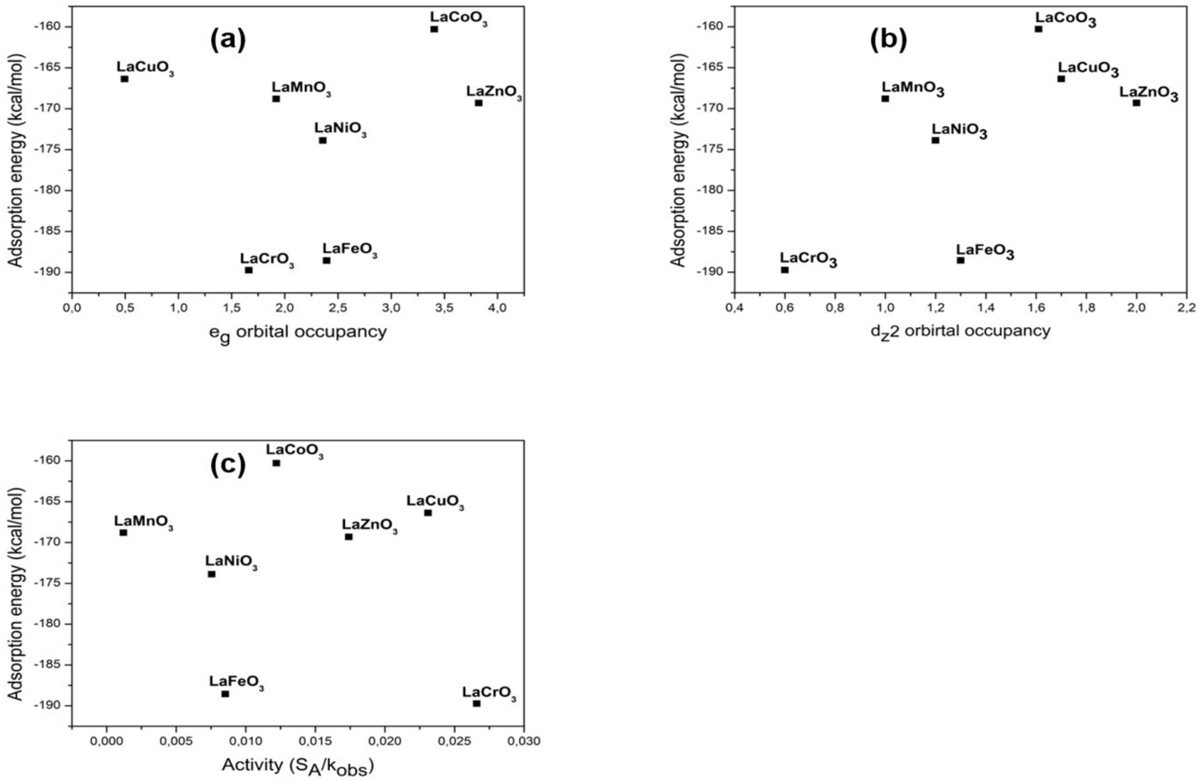

Figure S8: Plots of adsorption energy versus (a) catalytic activity (b) e_g orbital occupancy and (c) dz^2 orbital filling.

Adsorption energy: The energy, in kcal·mol^{-1}, released (or required) when the relaxed adsorbate components are adsorbed on the substrate. This is sum of the rigid energy and the deformation energy for the adsorbate components.

Rigid energy: The energy, in in kcal·mol^{-1}, released (or required) when the unrelaxed adsorbate components (before the geometry optimization step) are adsorbed on the substrate.

Deformation energy: The energy, in in kcal·mol^{-1}, released (or required) when adsorbate components are relaxed on the substrate surface.

Electronic structures of La-based perovskites

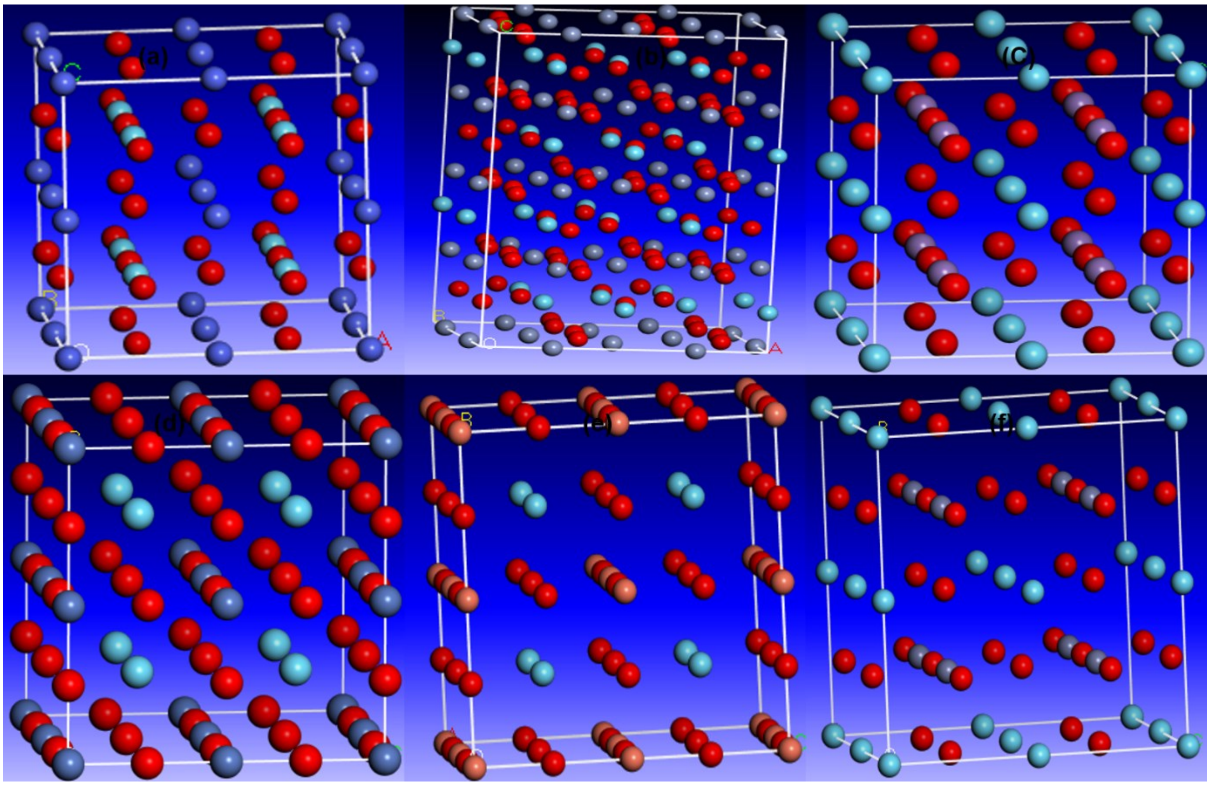

Figure S9: Optimized electronic structures of (a) $LaCoO_3$, (B) $LaCrO_3$, (c) $LaMnO_3$, (d) $LaNiO_3$, (e) $LaCuO_3$ and (f) $LaZnO_3$ perovskites.

References

[1] H. Xiao, R. Wang, L. Dong, Y. Cui, S. Chen, H. Sun, G. Ma, Biocompatible Dendrimer-Encapsulated Palladium Nanoparticles for Oxidation of Morin Biocompatible Dendrimer-Encapsulated Palladium Nanoparticles for Oxidation of Morin, ACS Omega. 4 (2019) 18685–18691. https://doi.org/10.1021/acsomega.9b02606.

[2] Z. Erlangung, Composites of Spherical Polyelectrolyte Brushes and Nanoparticles Synthesis , Characterization and Their Use in Catalysis, (2011).